J. Biomed. Eng. Res : 99-106, 2008

Time-Multiplexed RF Transmission to Improve B_1 Homogeneity in High Field MRI

Byung Hee Han, Jeung Hun Seo, Hye Young Heo, Soo Yeol Lee

Dept. of Biomedical Engineering, Kyung Hee University
(Received October 29, 2007. Accepted November 15, 2007)

Abstract

To improve B_1 homogeneity in high field MRI, the RF power is applied to the transmit array coil elements sequentially in the time-multiplexed way. Since only a single coil element is activated in a time-multiplexing slot, the global standing wave formation in the human body is greatly suppressed. The time-multiplexing slot width is on the order of micro seconds, hence, high-order-harmonic slices can be placed far from the transmit coil and simultaneous multiple slice selection can be avoided. The B_1 homogeneities of a birdcage coil and an eight-channel transmit array coil have been compared through finite difference time domain simulations. The simulation results indicate that the proposed technique can reduce the peak-to-peak B_1 inhomogeneity down to one fourth of the transmission with a birdcage coil on the central plane of the human head model at 3 T. The mimicking experiments at 3 T, eight separate experiments with a single coil element activated and image reconstruction by combining the eight images, also show promising results. It is expected that the proposed technique has some advantages over other B_1 improving methods in real practice since simple RF switching circuitries are only necessary and electromagnetic coupling between the coil elements is out of concern in its realization.

Key words : B_1 homogeneity, time-multiplexed transmission, transmit array coil, high field, dielectric effect

I. INTRODUCTION

Owing to its definite advantages in signal-to-noise ratio (SNR) and fMRI contrast, high field MRI is expected to play an important role in future MRI. The recent report on the preliminary human brain imaging at 9.4 T suggests that human head imaging is feasible at that high field strength [1]. It is believed that demands on higher spatial and spectral resolution in molecular or cellular MRI will necessitate development of even higher field MRI in the near future. However, high field MRI suffers from severe RF field (B_1) inhomogeneity coming from shortened electromagnetic wavelength in the human body at high frequency [2]. The B_1 inhomogeneity may result in contrast anomaly and improper measure of the physical quantities visualized by MRI.

Numerous methods have been proposed to mitigate the B_1 inhomogeneity in high field MRI. Among them are the introduction of specially designed RF coil configurations [3-6], the adiabatic RF pulses [7], the multi-dimensional tailored RF pulses [8-10], and the RF shimming with transmit coil array [11,12]. Recently, the transmit SENSE technique, originally devised to shorten the multi-dimensional RF pulse length in multi-dimensional spatial selection [13-16], has been also utilized for improving the B_1 homogeneity [17,18]. In the RF shimming technique, the magnitudes and phases of the RF currents in the transmit array coil elements are adjusted individually to produce uniform B_1 field in the target region. Therefore, the RF current shapes are the same in all the coil elements. In contrast, differently shaped RF pulses, each one designed considering the k-trajectory and the spatial sensitivity of the corresponding coil element, are fed to the transmit array coil elements in the transmit SENSE. It is believed that the transmit SENSE is more flexible than the RF shimming in improving B_1 homogeneity since the former has more degree of freedom in changing the RF and gradient waveforms. Recently, array-optimized composite pulse technique has been introduced to improve the flip angle homogeneity despite the inhomogeneous B_1 field of the transmit coil [19].

It seems that transmit array coils play key roles in improving the B_1 homogeneity in the future even though the transmit array coil complicates the RF hardware to a great extent. In the

This study was supported by a grant of the Korea Health 21 R&D Project, Ministry of Health and Welfare (02-PJ3-PG6-EV07-0002) and a grant from the Korea Science and Engineering Foundation (R11-2002-103).
Corresponding Author : Soo Yeol Lee, Ph.D.
Dept. of Biomedical Engineering, Kyung Hee University
1 Seochun, Kiheung, Yongin, Kyungki 446-701, Korea
Tel : +82-31-201-2980 / Fax : +81-31-201-3666
E-mail : sylee01@khu.ac.kr

RF shimming and transmit SENSE, it is essential to decouple the coil elements from each other sufficiently for the mathematical formulation to be valid in real practice. Therefore, decoupling the coil elements is one of the major problems in designing the transmit array coils. In this work, we propose a new technique to improve the B_1 homogeneity using the transmit array coils. Rather than applying continuous RF currents to each coil element, we apply chopped RF pulses sequentially to the coil elements in a time-multiplexed way to avoid the global formation of standing waves in the human subject. The B_1 homogeneity has been analyzed for an eight-channel transmit array coil at 3 T using the finite difference time domain (FDTD) method together with the consideration of specific absorption rate (SAR). Due to the lack of parallel RF transmission hardware, mimicking experiments, eight separate experiments with only a single coil element activated, have been performed at 3 T for the evaluation of the proposed technique with a phantom and human subjects.

II. MATERIALS AND METHODS

A. Time-Multiplexed RF Transmission to a Transmit Array Coil

When we use a single volume coil to transmit RF wave to a human subject, strong standing wave may be formed globally in the human subject, which often makes hot spots in the central region of the images at the field strength over 3.0 T. To avoid the global standing wave formation in transmitting with a transmit array coil, we apply chopped RF pulses to the coil elements in a time-multiplexed way as shown in Fig. 1. In a given time-multiplexing slot which is much shorter than the entire RF pulse length, only a single coil element receives the RF energy from the RF power amplifier with other coil elements disabled. Over the RF transmission period, every coil element receives the chopped RF pulses sequentially in its time slot in a time-multiplexed way. Phase shifters or delay lines should be placed in between the multiplexer and the coil elements to produce the rotating RF field with the transmit array coil. Since only a single coil element is activated in a given time slot, we expect weaker standing wave may appear in the local region around the activated coil element.

The time-multiplexed RF transmission can be implemented in a way similar to the RF shimming technique. The major difference is that the time-multiplexed technique uses chopped RF pulses rather than the continuous base-band RF pulses. Due to the chopping operation, the chopped RF pulse has high-order-harmonic components, which could select other slices than the desired base-band slice (central slice) at undesired positions. In Fig. 2, we have shown an example of the selection profile of a 90° chopped RF pulse. The original base-band RF pulse is an 8 ms-long Hamming-windowed sinc pulse with the slice-bandwidth of 1 kHz. The chopping frequency is 16 kHz with the time-multiplexing duty cycle of 1/8. The slice selection profile has been obtained by solving the Bloch equation. The slice bandwidth $\triangle f$ is determined by the envelope of the base-band RF pulse and the frequency interval between the harmonic slices is determined by the chopping frequency f_s. Therefore, we can control the slice thickness in the same way as in the conventional continuous RF pulse

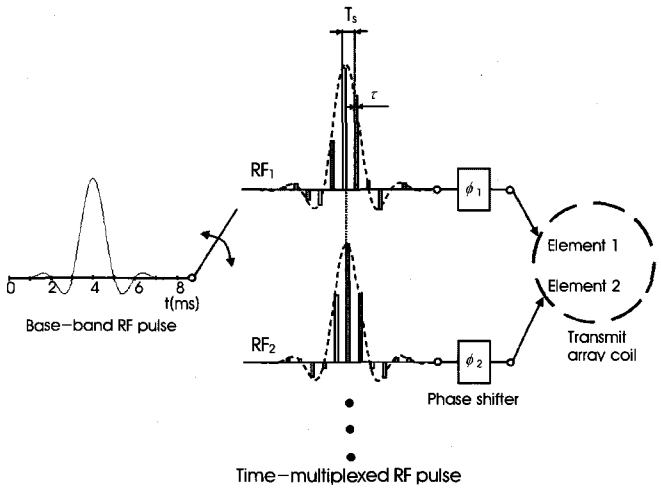

Fig. 1. Time-multiplexed RF transmission to the transmit array coil. Only a single coil element is activated in a given time slot.

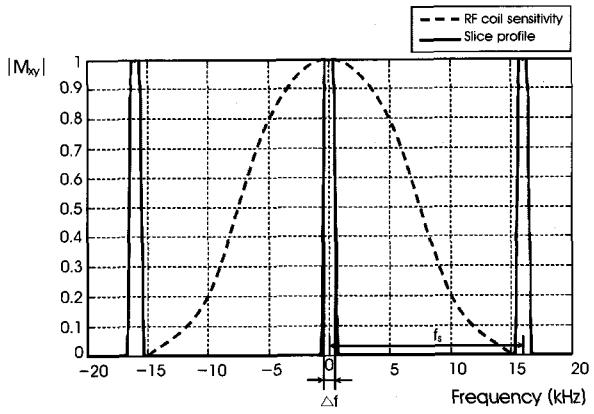

Fig. 2. The slice selection profile of the chopped RF pulse. The dashed line indicates the sensitive region of the transmit array coil. Only the base-band slice resides in the sensitive region and the other parasitic high-order-harmonic slices are outside the sensitive region.

transmission, and we can also control the harmonic slice interval by adjusting the chopping frequency. The central slice profile of the chopped RF pulse has been found to be virtually undistinguishable from the profile of the base-band RF pulse.

Among the multiple slices selected by the chopped RF pulses, only the central slice is desired. Therefore, the slices other than the central slice should be suppressed in the imaging. To suppress the signal from the high-order-harmonic slices, we utilize the sensitivity profile of the coil elements. By positioning the coil elements on top of the region of interest (ROI) and narrowing the coil width, we can limit the sensitive region around the central slice as shown in Fig. 2. If we make the chopping frequency high enough to move the high-order-harmonic slices far from the sensitive region, the slice selection at the far region can be avoided.

B. B_1 Homogeneity Evaluations

We calculated the B_1 fields by FDTD method using the XFDTD software (REMCOM Corp., State College, PA, USA). Aiming to use for human brain imaging, we designed an 8-channel transmit array coil as shown in Fig. 3. The four inner coil elements are mounted on a cylindrical surface with the diameter of 28 cm and the four outer coil elements on a cylindrical surface with the diameter of 32 cm. Each coil element has a rectangular shape which has the width of 12 cm and the span angle of $\varnothing$. The rather narrow width was chosen to limit the sensitivity region to the brain. Inside the transmit array coil model, we first placed a water-filled cylindrical phantom the diameter of 20 cm and the length of 24 cm. The dielectric constant and the conductivity of the water were assumed to be 78 and 0.15 S/m, respectively. The coil elements were made of 4 mm-wide thin copper strips and each coil element was tuned to 128 MHz. For the calculation of the transverse magnetization excited by the time-multiplexed transmission, we first calculated the sensitivity maps of all the coil elements. Upon the calculation of the sensitivity map of a coil element, the other coil elements were disabled by detuning them. After calculating the sensitivity maps, we multiplied the phase factors, e^{j0}, $e^{j\pi/4}$, $e^{j2\pi/4}$, $\cdots$, $e^{j7\pi/4}$, sequentially to the sensitivity maps to produce the rotating RF field inside the transmit array coil. We calculated the transverse magnetizations in each voxel using the following formula [20,21],

$$M_n = M_{n-1} + \gamma \int_{\tau} M_{n-1} \times B_{1n}^{+} \, dt \qquad (1)$$

where M_n is the magnetization after the n-th time-multiplexing slot, B_{1n}^{+} is the positive rotating B_1 field [22] of the coil element activated in the n-th time slot, τ is the time-multiplexing slot width, and γ is the gyromagnetic ratio. Initially, a unit vector M_0 is assumed in the z-direction and the T_1 and T_2 relaxation effects were excluded in the above calculation. Since the B_1 field felt by a voxel is weighted by the coil sensitivities in each time slot, the actual RF pulse waveforms are different among the voxels. Figure 4 shows examples of the B_1 pulse waveform at two different voxels in the water phantom when we use the sinc-shaped RF pulse. The solid line and dotted line represent the B_1 pulse waveforms at the center and at the periphery ($r = 0.8r_0$, r_0: phantom radius). The sensitivity maps were scaled so that the magnetization at the center of the phantom is flipped by 90°.

To make the transverse magnetization as homogeneous as possible, we found the optimal coil span angle by trial-and-

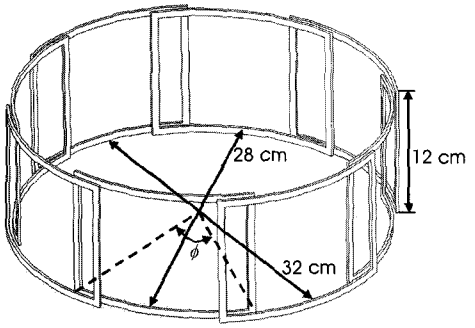

Fig. 3. The 8-element transmit array coil. The coil span angle ø is adjusted to improve the B1 homogeneity.

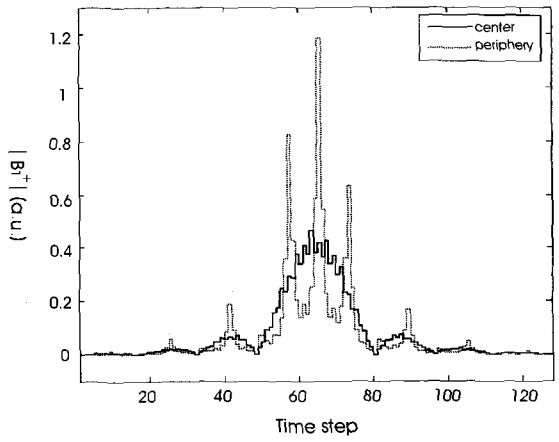

Fig. 4. The $|B_1^+|$ field waveform at the center (solid line) and a periphery (dotted line) of the phantom.

error approach. Since the RF transmission field distribution is dependent on what is inside the RF coil, it is not a simple matter to define the optimal span angle. For the given water cylinder, the optimal span angle $\varnothing$ has been found to be 53° at 128 MHz.

To compare the B_1 field homogeneity with that of a typical volume coil, we also calculated the B_1 field of the high-pass birdcage coil having 16 rungs. The birdcage coil has the diameter of 28 cm and the length of 26 cm. The rungs were made of 4 mm-wide thin copper strips. The birdcage coil was tuned to the same frequency of 128 MHz and the B_1 field was calculated with the same water cylinder loaded into the coil.

The B_1field homogeneity was also evaluated on the 3D digital human head model (REMCOM Corp., State College, PA, USA). The digital human head model consists of 17 different tissue types with $2\times2\times2.5mm^3$ spatial resolution. The electrical properties of the tissues were properly assigned at 128 MHz. The B_1sensitivity maps have been calculated for the human head model with the FDTD method, and the transverse magnetization maps have been calculated with the same procedure as in the water phantom case.

C. SAR Considerations

SAR has been also considered in the FDTD calculation. Since every coil element is activated in its exclusive time slots, the SAR of the transmit array coil can be calculated by simply adding the SARs of the individual transmit coil elements. In the time-multiplexed transmission, the relative SAR as compared to the birdcage coil transmission has been calculated as follows,

$$SAR_{total} = \frac{1}{N}\sum_{i=1}^{N}\left(\frac{w_{ta}}{w_{bc}}\right)^2 SAR_i \qquad (2)$$

in which w_{bc} and w_{ta} are the weighting factors to the sensitivity maps of the birdcage coil and the transmit array coil, respectively, to flip the magnetization by 90°at the center of the human head model, Nis the number of coil elements, and SAR_i is the SAR deposited to a given voxel by the i-th coil element in the transmit array coil.

D. Mimicking MRI Experiments

To evaluate the slice selection by the chopped RF pulse, we made a cylindrical water phantom as shown in Fig. 5. The phantom has 16 cm-long acrylic cylinders on both sides to observe any multiple slice selection by the high-order-harmonics of the chopped RF pulse when the central region of the phantom is imaged. The phantom was filled with saline solution.

For the time-multiplexed transmission, we made the8-element transmit coil array derived from the FDTD simulation. The coil was made of 4 mm-wide copper strips. Each coil element was divided into four sections between which capacitors were connected for tuning. To compare the B_1 homogeneity, we used a birdcage coil with the diameter and length of 28 cm and 26 cm, respectively. The birdcage coil was the high-pass type having 16 rungs.

Since only a single RF transmission channel is currently available in our 3 T system, we performed mimicking experiments, that is, eight separate experiments each time with a single coil element activated and the others detuned. After acquiring MRI signals from all the coil elements, we added the MR images from every coil element together in the complex domain to get final images. Since the transverse magnetization should be obtained considering the vector nature of the interm-ediate magnetization during the time-multiplexed transmission as implied in Eq. [1], the experimental results should be different from the simulation results. However, we believe this mimicking experiment may demonstrate the feasibility of the proposed techniquein some extent. It has been reported that the result of parallel excitation can be estimated from the superposition of the images observed from the mimicking single-channel experiments in the small-tip-angle excitation regime [13,15]. In the mimicking experiments, we synthesized the chopped RF pulse in the spectrometer, rather than switching the RF power amplifier output, due to the lack of RF switching devices. The chopped RF pulses were fed to the modulator circuit to shift the center frequency of the RF pulse to 128 MHz. For the base-band RF pulse, we used a Hamming-windowed sinc pulse having the slice-bandwidth of 1 kHz and the pulse length of 8 ms. The chopping frequency was 32 kHz which made the interval between the base-band slice and the first-harmonic slice be 16 cm when the slice thickness was 5 mm.

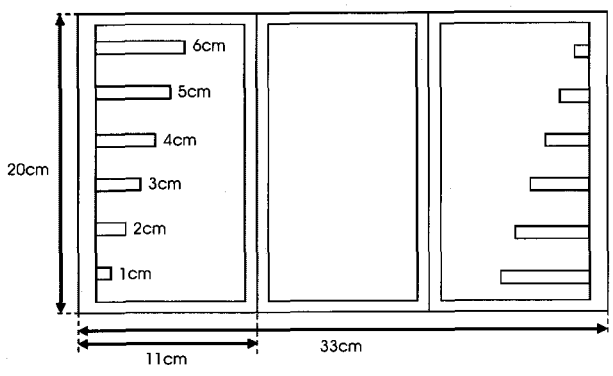

Fig. 5. The water phantom to evaluate the slice selection performance.

III. RESULTS

Figure 6a and 6b show the calculated transverse magnetization on the central plane of the water phantom when the spins were excited by the birdcage coil and the transmit array coil, respectively. In both cases, the spins at the center of the water phantom were excited by 90°. Figure 6b was obtained with the time-multiplexed transmission while Fig. 6a was obtained with the base-band transmission. The birdcage coil image shows the typical hot spot at the central region, however, the hot spot is mitigated in the transmit array coil image. The standard deviations of the transverse magnetization are 15% and 5% in Fig. 6a and Fig. 6b, respectively. The peak-to-peak inhomogeneities of the transverse magnetization in the same figures are 50.4% and 18.3%, respectively. For the mimicking MRI experiments, we used the water phantom shown in Fig. 5 and the gradient echo sequences with TR/TE of 300/15 ms. To compare the B_1 homogeneity between the transmit array coil using the time-multiplexed RF pulse and the birdcage coil using the base-band RF pulses, we obtained the water phantom images using the birdcage coil with the same imaging parameter. The amplitude of the time-multiplexed RF pulse was determined so that the central region has the desired flip angle of 90°. The birdcage coil had been driven in a quadrature mode to improve the B_1 homogeneity. Figure 6c and 6d show the central plane images taken with the birdcage coil and the transmit array coil, respectively. The birdcage coil shows the peak-to-peak inhomogeneity of 87.8%, while the transmit coil array shows only 38.4%. The standard deviations of the pixel intensities in Fig. 6c and 6d are 49.7% and 13.9%, respectively.

Figure 7a and 7b show the calculated transverse magnetization maps on the central plane of the human head model when the spins are excited by the base-band transmission with the birdcage coil and the time-multiplexed transmission with the transmit array coil, respectively. In Fig. 7c and 7d, the relative SAR maps are shown for the birdcage coil and the transmit array coil, respectively. The standard deviations of the transverse magnetization on the central plane of the human head model are 4.6%and 0.9% for the birdcage coil and the transmit array coil, respectively. The peak-to-peak inhomogeneities of the transverse magnetization on the sameplane are 20.6% and 4.7% for the birdcage coil and the transmit array coil, respectively. In the 6 cm thick central slab in the human head model, the peak-to-peak inhomogeneity and the standard deviation of the transverse magnetization decreased from 21.1% to 8.1% and from 4.6% to 1.4%, respectively, by utilizing the time-multiplexed transmission. However, the peak 1g SAR of the transmit array coil on the central slice increased by 2.6 times as compared to that of the birdcage coil. In the 6 cm thick central slab, the peak 1g SAR of the transmit array coil increased 2.3 times as compared to that of the birdcage coil. From Fig. 7d, we can notice that 1g SAR is relatively high in the periphery of the human head model. At a voxel in the

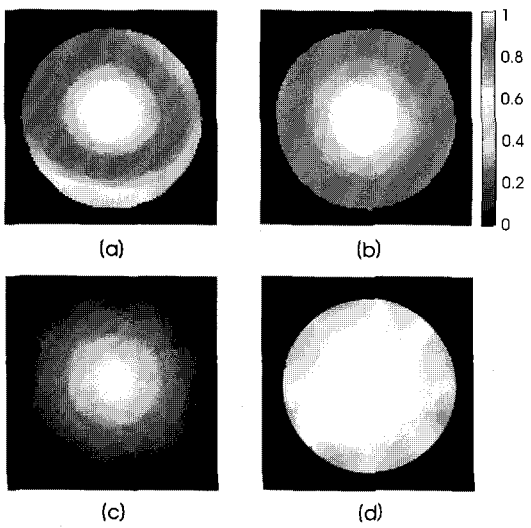

Fig. 6. The calculated transverse magnetization maps for(a) the birdcage coil and (b) the transmit array coil at the central plane of the water phantom (z=0) at 128 MHz. (c) and (d) are the gradient echo images of the water phantom taken with the birdcage coil and the transmit array coil, respectively.

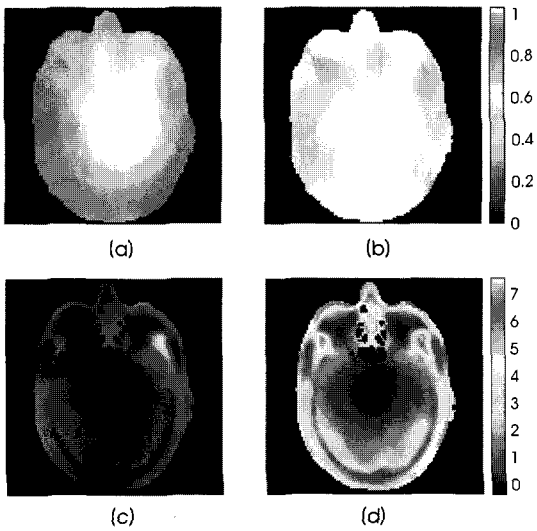

Fig. 7. The calculated transverse magnetization maps for (a) the birdcage coil and (b) the transmit array coil at the central plane of the human head model (z=0) at 128 MHz. (c) and (d) are the corresponding relative 1g SAR maps of the birdcage coil and the transmit array coil, respectively.

peripheral region, most of RF energy is received from the nearby coil elements, hence, the RF pulse waveform at a peripheral voxel is more chopped than the one at a central voxel as can be noticed from Fig. 4. Therefore, the RF pulse in the peripheral region has stronger high-order-harmonics than in the central region, resulting in higher SAR in the peripheral region.

In order to compare the slice selection imaging performance, we used the water phantom shown in Fig. 5. We first took the gradient echo images of the water phantom with TR/TE of 300/15 ms by the time-multiplexed RF pulses. To evaluate the slice selection performance, we also took multi-slice gradient echo images with the base-band RF pulsewith all the imaging parameters kept the same as in the time-multiplexed experiments except the RF pulse amplitude. Figure 8a shows the eight gradient echo images of the central plane taken with each element of the transmit array coil driven by the base-band RF pulse. Figure 8b shows the eight gradient echo images of the same plane taken with the time-multiplexed RF pulse. The slice thickness is 5 mm with no slice gaps and the interval between the adjacent harmonic slices is 16 cm with the chopping frequency of 32 kHz. The combined images are shown at the right-hand side of the images. Since the high-order-harmonic slices are far from the central region, the combined image taken with the time-multiplexed RF pulse shows no noticeable signals from the high-order-harmonic slices. Figure 9a and 9b show brain images of a human subject obtained with the birdcage coil and the transmit array coil, respectively. The images have been taken with the gradient echo sequence with TR/TE of 300/15 ms. The slice thickness was 5mmwith no slice gaps and the number of slices was 10. We used the same time-multiplexed RF pulses as the one used in the water phantom imaging.

IV. DISCUSSIONS AND CONCLUSIONS

The proposed technique improves the B_1 homogeneity in both water phantom and human head models with increase of SAR in the periphery of the models. In the central region of the human head model, the SAR of the transmit array coil is maintained at the similar level of the birdcage coil. Even though the effective RF pulse length in acoil element is shortened by factor of the number of coil elements due to the time-multiplexing, SAR is not necessarily increased by the same factor. The RF pulse waveform felt by the spins at the central region is similar tothe based-band waveform, as can be noticed from Fig. 4, since the spins at the central region always receive similar RF energies from all of the transmit coil elements. Therefore, it can be said that the SAR deposited by the transmit array coil may not be very different from the one deposited by the single volume coil in the central region. However, the increase of SAR in the peripheral region is inevitable in the proposed technique. It is reported that simultaneous transmission of RF pulse through multiple coils may cause their electric field interact constructivelyresulting in significant increase of SAR in the parallel transmission [23-25]. Since SAR is one of the important issues in transmit array coil experiments [26,27], we must investigate the SAR

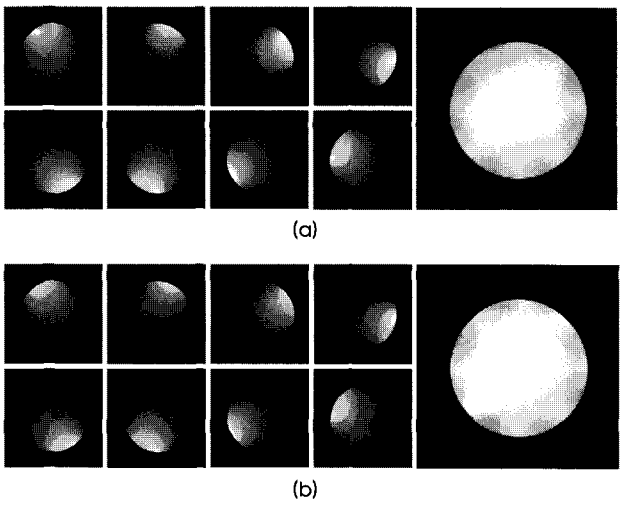

Fig. 8. The phantom images taken with a single element of the transmit array coil with (a) the base-band continuous RF pulse and (b) the time-multiplexed chopped RF pulse. The right-hand side images are combined images.

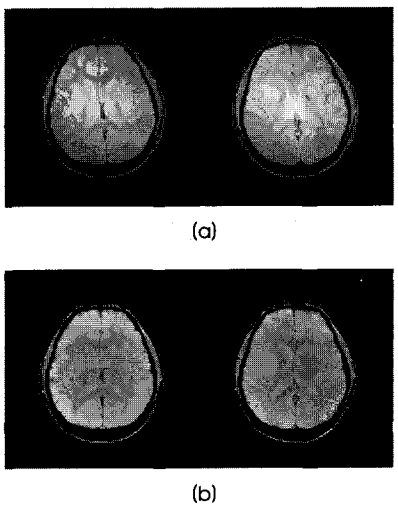

Fig. 9. The human brain images taken with (a) the birdcage coil and (b) the transmit array coil, respectively (TR/TE = 300/15 ms).

effect further in terms of the number of coil elements and coil element shape.

In this study, we only considered a special case in which the number of coil elements is eight and the field strength is 3 T. Recent studies are focused on higher field strength over 7 T. We need to extend this study to higher field strength using variety of transmit coil configurations. It is believed that more coil elements are necessary at higher fields to secure acceptable B_1 homogeneity. Recent simulation studies suggest that at least 16 elements are necessary at 7 T and 80 elements at 14 T if the RF shimming technique is used to secure the B_1 homogeneity [11].

With the mimicking experiments, we have demonstrated the feasibility of the proposed technique. Since the brain images in Fig. 9b have been obtained by combining the eight separate images, T_1-contrast of the combined images should be different from the ones taken with truly parallel excitation in the time-multiplexed way. Therefore, we still need to verify the proposed technique further with truly time-multiplexing excitation. We are now developing the RF hardware, RF power dividers and switching circuitries, for the experiments. We expect the proposed technique can be realized with much simpler RF hardware than is necessary in other techniques using a transmit array coil.

In conclusion, the time-multiplexed RF transmission with a transmit array coil can improve the B_1 homogeneity at 3 T as compared to the typical volume coil with increase of SAR in the peripheral region of the subject.

REFERENCES

[1] T. Vaughan, L. DelaBarre, C. Snyder, J. Tian, C. Akgun, D. Shrivastava, W. Liu, C. Olson, G. Adriany, J. Strupp, P. Andersen, A. Gopinath, P.-F. van de Moortele, M. Garwood, and K. Ugurbil, "9.4T human MRI: preliminary results," *Magn. Reson. Med.*, vol. 56, pp. 1274-1282, 2006.

[2] P. Bottomley, and E. Andrews, "RF magnetic field penetration, phase shift and power dissipation in biological tissue: implications for NMR imaging," *Phys. Med. Biol.*, vol. 23, pp. 630-643, 1978.

[3] J.T. Vaughan, H.P. Hetherington, J.O. Out, J.W. Pan, and G.M. Pohost, "High frequency volume coils for clinical NMR imaging and spectroscopy," *Magn. Reson. Med.*, vol. 32, pp. 206-218, 1994.

[4] D.C. Alsop, T.J. Connick, and G. Mizsei, "A spiral volume coil for improved RF field homogeneity at highstatic magnetic field strength," *Magn. Reson. Med.*, 1998;40:4954.

[5] T.S. Ibrahim, R. Lee, B.A. Baertlein, A.M. Abduljalil, H. Zhu, and P.L. Robitaille, "Effect of RF coil excitation on field inhomogeneity at ultra high fields: a field optimized TEM resonator," *Magn. Reson. Imag.*, vol. 19, pp. 1339-1347, 2001.

[6] J.T. Vaughan, G. Adriany, C.J. Snyder, J. Tian, T. Thiel, L. Bolinger, H. Liu, L. DelaBarre, and K. Ugurbil, "Efficient high-frequency body coil for high-field MRI," *Magn. Reson. Med.*, vol. 52, pp. 851859, 2004.

[7] S. Conolly, D. Nishimura, and A. Macovski, "A selective adiabatic spin-echo pulse," *J. Magn. Reson.*, vol. 83, pp. 324-334, 1989.

[8] R. Deichmann, C.D. Good, and R. Turner, "RF inhomogeneity compensation in structural brain imaging," *Magn. Reson. Med.*, vol. 47, pp. 398-402, 2002.

[9] S. Saekho, F.E. Boada, D.C. Noll, and V.A. Stenger, "Small tip angle three-dimensional tailored radiofrequency slab-select pulse for reduced B_1 inhomogeneity at 3T," *Magn. Reson. Med.*, vol. 53, pp. 479-484, 2005.

[10] S. Saekho, C. Yip, D.C. Noll, F.E. Boada, and V.A. Stenger, "Fast-kz three-dimensional tailored radiofrequency pulse for reduced B_1 inhomogeneity," *Magn. Reson. Med.*, vol. 55, pp. 719-724, 2006.

[11] W. Mao, M.B. Smith, and C.M. Collins, "Exploring the limits of RF shimming for high-field MRI of the human head," *Magn. Reson. Med.*, vol. 56, pp. 918922, 2006.

[12] C.M. Collins, W. Liu, B.J. Swift, and M.B. Smith, "Combination of optimized transmit arrays and some receive array reconstruction methods can yield homogeneous imagesat very high frequencies," *Magn. Reson. Med.*, vol. 54, pp. 1327-1332, 2005.

[13] Y.D. Zhu, "Parallel excitation with an array of transmit coils," *Magn. Reson. Med.*, vol. 51, pp. 775-784, 2004.

[14] P. Ullmann, S. Junge, M. Wick, F. Seifert, W. Ruhm, and J. Hennig, "Experimental analysis of parallel excitation using dedicated coil setups and simultaneous RF transmission on multiple channels," *Magn. Reson. Med.*, vol. 54, pp. 994-1001, 2005.

[15] U. Katscher, P. Börnert, C. Leussler, and J.S. van den Brink, "Transmit SENSE," *Magn. Reson. Med.*, vol. 49, pp. 144-150, 2003.

[16] U. Katscher, P. Börnert, and J.S. van den Brink, "Theoretical and numerical aspects of transmit SENSE," *IEEE Trans. Med. Imaging*, vol. 23, pp. 520-525, 2004.

[17] K. Setsompop, L.L. Wald, V. Alagappan, B. Gagoski, F. Hebrank, U. Fontius, F. Schmitt, and E. Adalsteinsson, "Parallel RF transmission with eight channels at 3 Tesla," *Magn. Reson. Med.*, vol. 56, pp. 1163-1171. 2006.

[18] Z. Zhang, C.-Y. Yip, W. Grissom, D.C. Noll, F.E. Boada, and V. A. Stenger, "Reduction of transmitter B_1 inhomogeneity with transmit SENSE slice-select pulses," *Magn. Reson. Med.* vol. 57, pp. 842-847, 2007.

[19] C.M. Collins, Z. Wang, W. Mao, J. Fang, W. Liu, and M.B. Smith, "Array-optimized composite pulse for excellent whole-brain homogeneity in high-field MRI," *Magn. Reson. Med.*, vol. 57, pp. 470-474, 2007.

[20] C.M. Collins, B.L. Beck, J.R. Fitzsimmons, S.J. Blackband, and M.B. Smith, "Strengths and limitations of pulsing coils in an array sequentially to avoid RF interference in high field MRI," in *Proc.13th Annual Meeting of ISMRM*, Miami Beach, FL, USA, 2005, Abstract 816.

[21] C.M. Collins, Z. Wang, W. Mao, J. Fang, W. Liu, G. Adriany, J.T. Vaughan, K. Ugurbil, and M.B. Smith, "Multi-coil composite pulses for whole-brain homogeneity improved over RF shimming alone," in *Proc.14th Annual Meeting of ISMRM*, Seattle, USA, 2006, Abstract 702.

[22] D.I. Hoult, "The principle of reciprocity in signal strength calculations-A mathematical guide," *Concepts Magn. Reson.*, vol. 12, pp. 173-187, 2000.

[23] J. Wang, S.H. Oh, M.B. Smith, and C.M. Collins, "RF shimming considering both excitation homogeneity and SAR," in *Proc. 15th Annual Meeting of ISMRM*, Berlin, Germany, 2007, Abstract 1022.

[24] A.C. Zelinski, V.K. Goyal, L. Angelone, G. Bonmassar, L.L. Wald, and E. Adalsteinsson, "Designing RF pulses with optimal specific absorption rate (SAR) characteristics and exploring excitation fidelity, SAR and duration tradeoffs," in *Proc. 15th Annual Meeting of ISMRM*, Berlin, Germany, 2007, Abstract 1699.

[25] X. Wu, C. Akgun, J.T. Vaughan, K. Ugurbil, P.F. Van de Moortele, "SAR analysis for transmit SENSE at 7T with a human head model," in *Proc. 15th Annual Meeting of ISMRM*, Berlin, Germany, 2007, Abstract 3350.

[26] W. Mao, Z. Wang, M.B. Smith, and C.M. Collins, "Calculation of SAR for transmit coil arrays," *Concepts Magn. Reson. Part B*, vol. 31B, pp. 127-131, 2007.

[27] C.A.T. Van den Berg, B. Van den Bergen, J.B. Van de Kamer, B.W. Raaymakers, H. Kroeze, L. Bartels, J.J. Lagendijk, "Simultaneous B_1+ homogenization and specific absorption rate hotspot suppression using a magnetic resonance phase array transmit coil," *Magn. Reson. Med.*, vol. 57, pp. 577-586, 2007.